Biophys. Struct. Mech. 2, 159–180 (1976)

Biophysics of Structure and Mechanism

Dynamics of the Aromatic Amino Acid Residues in the Globular Conformation of the Basic Pancreatic Trypsin Inhibitor (BPTI)

II. Semi-Empirical Energy Calculations

Robert Hetzel[1], Kurt Wüthrich[1], Johann Deisenhofer[2], and Robert Huber[2]

[1] Institut für Molekularbiologie und Biophysik, Eidgenössische Technische Hochschule CH-8093 Zürich-Hönggerberg, Switzerland

[2] Abteilung Strukturforschung II, Max Planck-Institut für Biochemie D-8033 Martinsried bei München, Federal Republic of Germany

Summary. The molecular conformation of the basic pancreatic trypsin inhibitor (BPTI) is known in considerable detail from both X-ray studies in single crystals and NMR studies in solution. The NMR experiments showed that the aromatic rings of the phenylalanyl and tyrosyl residues can undergo rapid rotational motions about the C^{β}–C^{γ} bond. The present paper describes a model investigation of the mechanistic aspects of these intramolecular rotational motions. From calculations of the conformational energies for molecular species derived from the X-ray structure by rotations of individual aromatic rings, it was apparent that the rotational motions of the aromatics could only be understood in a flexible structure. Flexibility was simulated by allowing the protein to relax to an energetically favorable conformation for each of the different rotation states of the aromatic rings. It was then of particular interest to investigate how the perturbations caused by different rotation states of the aromatic rings were propagated in the protein structure. It was found that the rotation axes C^{β}–C^{γ} were only slightly affected ($\Delta\chi^1 \lesssim 20°$). The most sizeable perturbations are caused by through space interactions with nearby atoms, which move away from the ring center and thus release the steric hindrance opposing the rotational motions. The values for the energy barriers obtained from the energy minimization are of the same order of magnitude as those measured by NMR.

Key words: Conformational energy calculations – Protein conformation – Molecular mechanics – Proteinase inhibitor.

Introduction

With the presently available experimental data on the molecular conformation of the basic pancreatic trypsin inhibitor (BPTI), this protein lends itself to rather detailed comparisons of the spatial structures in the crystalline form and in solution. For BPTI single crystals, a molecular model was derived from the X-ray data (Huber et al., 1971), and extensive use of refinement techniques was made in the analysis at 1.5 Å resolution (Deisenhofer and Steigemann, 1975). From the small temperature coef-

ficients it can be concluded that crystalline BPTI represents a comparatively well defined and rather rigid spatial protein structure. Aqueous solutions of BPTI were studied extensively by NMR techniques. As was shown in the preceding paper I (Wagner et al., 1976), the conformation of BPTI in aqueous solution is very similar to that in the single crystals, and the backbone structure is outstandingly rigid over the temperature range from approximately 4°–87°. Yet it was also observed that in the rigid skeleton of the molecule most of the aromatic rings of the phenylalanyl and tyrosyl residues were rotating rapidly about the C^{β}–C^{γ} bond. The present paper describes mechanistic aspects of these intramolecular rotational motions. These were investigated on the basis of semi-empirical energy calculations for molecular species derived from the X-ray structure of BPTI either by rotations of the aromatic rings about the C^{β}–C^{γ} bond, or by replacement of aromatic rings with equivalent spheres respresenting the space temporarily occupied during a rotation by 360°.

The following characteristics of the BPTI molecule will frequently be mentioned throughout the paper. BPTI is a small protein consisting of one polypeptide chain with 58 amino acid residues. The amino acid sequence includes four tyrosyl residues in the positions 10, 21, 23 and 35, and four phenylalanyl residues in the positions 4, 22, 33 and 45. Overall the amino acid composition is such that the molecule comprises 454 "heavy atoms", i.e. carbon, nitrogen, oxygen and sulfur atoms.

It is readily apparent in the rigid X-ray structure of BPTI, that the aromatic rings could not rotate about the C^{β}–C^{γ} bonds because of near interatomic contacts with the surrounding amino acid residues. This followed also from an independent investigation of Gelin and Karplus (1975). In the following we will therefore concentrate on "flexible" BPTI structures, in which the protein was allowed to relax to energetically favored structures for the different rotation states of the aromatic rings. In the analysis of the results thus obtained, the main emphasis was on studies of the propagation in the protein structure of the perturbations caused by the ring rotations. The energy minimization procedures further yielded values for the barriers to rotational ring motions, which will be compared with the experimental values obtained from NMR studies (Wagner et al., 1976).

Molecular Models and Methods

The calculations reported in this paper were based on the single crystal conformation of BPTI. With the use of suitable molecular models, the X-ray structure was then modified so that the conformational energies of species including different rotation states of the individual aromatic rings could be investigated. This section includes a description of relevant features of the X-ray structure and two different models used to study non-equilibrium rotational states of the aromatic rings, i.e. the "sphere model" and the "ring model", and presents the conformational energy function and the techniques used for energy refinement of the molecular models.

The Single Crystal X-Ray Structure (X)

The first single crystal conformation of BPTI was obtained by Huber et al. (1971) from X-ray crystallographic data at a resolution of 2.5 Å. Deisenhofer and Steige-

mann (1975) expanded these data to 1.5 Å resolution and refined the model by a constrained crystallographic refinement method. This technique consisted of a cyclic application of the real space refinement of Diamond (1971) against electron density maps computed with the experimental structure factor amplitudes and the phases calculated from the molecular model obtained in the preceding cycle. Using Fourier difference maps, these authors were also able to locate a number of solvent molecules in the crystal structure of BPTI. In the present investigations we deal exclusively with the isolated BPTI molecule, without considering the solvent molecules or neighboring protein molecules of the crystal lattice. The isolated BPTI molecule in the conformation of Deisenhofer and Steigemann (1975) will in the following be referred to as the "X-ray structure", or simply as "X".

Some properties of the crystallographic refinement techniques used by Deisenhofer and Steigemann (1975) are of particular relevance for the present investigation, especially in view of some principal differences to the energy refinement method described below. The most important point is that the refinement bases entirely on the measured X-ray intensities. The rigid-body refinement procedure makes use of amino acid geometries determined by small molecule X-ray crystallography. Primarily, rotations about single bonds are allowed. In addition, the interbond angles $\tau(\mathrm{NC}^{\alpha}\mathrm{C}')$ and the ω torsion angles about the peptide bonds were varied. The steric strain which occurs in individual segments of the polypeptide backbone tends to concentrate in these angles. No explicit checks for short non-bonded contacts were carried out, as it was assumed that the overdetermination (ratio of measurements and variables) was sufficiently large to rely solely on the X-ray data.

Calculations of the Conformational Energy

A set of procedures developed by Levitt and Lifson (1969) and by Levitt (1974) was used for all the conformational energy calculations and energy refinements reported in this paper. In these methods, the conformational energy of a protein is assumed to be a simple empirical function (1) of the relative positions of the individual non-hydrogen atoms:

$$E = \sum_{\text{bonds}} \tfrac{1}{2} K_b (b_i - b^0)^2 + \sum_{\substack{\text{bond}\\ \text{angles}}} \tfrac{1}{2} K_\tau (\tau_i - \tau^0)^2 + \sum_{\substack{\text{torsion}\\ \text{angles}}} K_\theta \{1 + \cos(m\theta_i + \delta)\} + \sum_{\substack{\text{non-bonded}\\ \text{distances} < R_{\max}}} \{A/r_{ij}^{12} + B/r_{ij}^{6}\}. \quad (1)$$

K_b are the bond stretching force constants, K_τ the bond angle bending force constants, b^0 the equilibrium bond lengths and τ^0 the equilibrium bond angles. K_θ are the barriers for torsional motions about interatomic bonds, and m and δ are the periodicity and the phase of these barriers. A and B are the repulsive non-bonded parameters and the long range non-bonded parameters, respectively. Non-bonded interactions were calculated between all pairs of atoms which are separated by at least three bonds and are closer together than a cut-off separation $R_{\max}$. The presence of the hydrogen atoms is not explicitely considered, but is accounted for by the energy parameters used for the heavy atoms to which they are attached.

For computations of the contributions to the conformational energy which did not involve direct interactions with aromatic rings in non-equilibrium rotation states, the energy function (1) was used with the energy parameters suggested by Levitt (1975). The non-bonded parameters A and B, the torsional potential parameters K_θ, m and δ, the equilibrium bond lengths b^0 and the equilibrium bond angles τ^0 are essentially identical to those given in the Tables 2, 3, 5, 7 and 8 of the paper by Levitt (1974), whereas the values used for the force constants K_b and K_τ are somewhat different from those given in the Table 4 and 6 of the same paper (Levitt, 1974). Many of these parameters, e.g. B, b^0 and τ^0, had been evaluated empirically from the real space refined X-ray structure of Lysozyme (Diamond, 1974). In particular, Levitt evaluated the non-bonded parameters B empirically from this structure in an attempt to account in a qualitative way for hydrogen bonding and for hydrophobic interactions; e.g. for the interaction of a carbonyl oxygen with a hydroxyl group, the non-bonded potential $(A/r^{12} + B/r^6)$ has a minimum of -1.1 kcal mole^{-1} for $r = 2.9$ Å, whereas the corresponding values for two interacting carbonyl oxygens are -0.007 kcal mole^{-1} and 4.4 Å. In principle, these empirical parameters could for the present investigations have been redetermined from the X-ray structure of BPTI; for practical reasons we preferred to use the values given by Levitt (1975) for all the energy parameters.

Energy Refinement of the Molecular Structures

For the energy refinements, procedures by Levitt (1974, 1975) were used. This method is primarily designed for refinements of protein conformations obtained from X-ray diffraction studies, mainly by improving the stereochemistry of these conformations; steric strain encountered in the original molecular model is distributed evenly throughout the whole molecule. This is achieved by variation in small steps of the positions of all the atoms in such a way that the conformational energy obtained by evaluating the energy function (1) decreases. This procedure is repeated in a sufficient number of consecutive cycles to obtain a stereochemically acceptable structure. It is an inherent characteristic of this method, which will also be manifest in some of the results on BPTI, that it attempts to find a minimum of the energy function (1) for a conformation which does not in any of the local structural features deviate drastically from the initial model conformation.

Application of these procedures to the X-ray structure of BPTI gave the energy refined X-ray structure ref X (Table 2). The techniques of Levitt were also used to investigate the behavior of BPTI conformations which had been derived from the X-ray structure by rotation of individual aromatic rings about the C^β–C^γ bond. The idea was to consider non-equilibrium rotation states of the aromatic rings as small perturbations of the X-ray conformation, and to use energy refinement to mimic the flexibility of the protein in reacting to these perturbations. From this we expected to get some insight into the nature of the intramolecular fluctuations of BPTI which remove part of the steric hindrance to ring rotation which is characteristic of the rigid models.

In the application to BPTI, the energy function was minimized by the method of steepest descent in the (3×454 dimensional) configuration space of all atomic

coordinates in the molecule. The length of the step down the gradient is adjusted automatically; only an initial step length must be given. In this work, an initial root mean square step of 0.03 Å was chosen. Since the minimization method is not quadratically convergent, the refinement process had to be interrupted after an arbitrary number of cycles, long before the energy minimum was reached; in practice, all minimizations were stopped after 100 cycles. By this time the stereochemistry was rather good in all the species considered, and the energy difference ΔE changed very slowly, i.e. in the mean by $\lesssim 0.1$ kcal mole^{-1} per cycle; the absolute conformational energies E still decreased at a mean rate of about 0.4 kcal mole^{-1} per cycle.

The Sphere Model

With the sphere model we attempt to mimic the perturbations of the molecular conformation caused by the combined effects of all the rotational states of one aromatic ring. This treatment should somewhat overestimate the energy barriers, and possibly also the intramolecular motions of neighboring atoms induced by the rotating ring.

The model is based on the observation (see Fig. 3) that the hindrance to rapid ring rotation in the rigid protein environment is mainly due to short non-bonded interatomic contacts encountered by ring atoms in intermediate rotational states. These strong non-bonded repulsions can best be visualized in terms of a description where the atoms are taken to be spheres of fixed radii which are not allowed to overlap. Each atom thus takes up a certain volume of the space occupied by the protein molecule. In this scheme, the aromatic rings can be represented as circular disks, and the volume occupied by the ensemble of all the rotational states of an aromatic ring about the C^β–C^γ bond is approximately spherical in shape. In the sphere model we replaced the aromatic rings, including the η-oxygen atom in the case of tyrosine, by equivalent spheres which occupy approximately the same volume as the above mentioned ensemble of rotational states. In the energy calculations and energy refinements, this sphere was then treated like a single atom of a new atomic type Y, thus representing the simultaneous presence of all rotational states of a given ring.

The rigid sphere model structures $S[i]$ (Table 2) were derived from the X-ray structure by positioning the equivalent spheres replacing the aromatic ring atoms C^γ_i, $C^{\delta_1}_i$, $C^{\delta_2}_i$, $C^{\varepsilon_1}_i$, $C^{\varepsilon_2}_i$, C^ζ_i, and – in the case of tyrosine – O^η_i on the extension of the C^β_i–C^γ_i bond at a distance of 2.9 Å from the C^β_i atom. This position coincides within approx. 0.05 Å with the center of the aromatic rings studied. For the energy calculations in the model structures $S[i]$, we used the energy function (1) and, in as far as no interactions with the spheres Y were concerned, the energy parameters discussed before (Levitt, 1975). For all interactions involving the spheres Y, i.e. C^β–Y bond stretching, C^α–C^β–Y bond angle bending and non-bonded interactions of the spheres Y with all the other atoms in the protein molecule, new energy parameters had to be determined: From CPK molecular models we estimated two radii for the sphere Y, i.e. a "van der Waals radius" $r_{\mathrm{vdW}}(\mathrm{Y}) = 3.5$ Å and an extreme short contact radius $r_{\mathrm{ex}}(\mathrm{Y}) = 2.8$ Å. $R_{\mathrm{ex}}(\mathrm{Y}\,..\,\mathrm{X})$, the extreme short contact distance be-

tween an atom of type X and the sphere Y (Table 1), was computed to be approximately

$$R_{ex}(Y\,..\,X) = r_{ex}(Y) + \tfrac{1}{2} \cdot R_{ex}(X\,..\,X), \tag{2}$$

where $R_{ex}(X\,..\,X)$ was taken from Table 8 of Levitt (1974). The values for $r_{vdW}(Y)$ and $R_{ex}(Y\,..\,X)$ were then used to determine the cut-off separations R_{max} and the non-bonded repulsive parameters A (Table 1) with the methods described by Levitt (1974). B was set to zero for all non-bonded interactions involving the sphere Y (Table 1). Furthermore, as mentionned above, b^0 for the C^β—Y bond was fixed at 2.9 Å; for $K_b(C^\beta—Y)$, the value given by Levitt (1975) for the $C^\beta—C^\gamma$ bond was used; for $K_\tau(C^\alpha—C^\beta—Y)$ and $\tau^0(C^\alpha—C^\beta—Y)$, the values given by Levitt (1975) for the bond angle $C^\alpha—C^\beta—C^\gamma$ were adopted.

Table 1. Energy parameters for non-bonded interactions with the sphere Y replacing the aromatic rings in the sphere model

Type of interaction[a]	A (10^6 kcal mole^{-1} Å^{-12})	B (kcal mole^{-1} Å^{-6})	R_{max} (Å)	R_{ex} (Å)
Y . . . O	154	0	7.10	4.1
Y . . . N	154	0	7.15	4.1
Y . . . C	286	0	7.35	4.3
Y . . . A	211	0	7.25	4.2
Y . . . S	286	0	7.35	4.3

[a] The symbol Y stands for the equivalent sphere replacing the aromatic ring in the sphere model calculations; O stands for oxygen, N for nitrogen, C for tetravalent carbon, A for trivalent carbon and S for sulphur

Table 2. The molecular models of BPTI considered in this paper

Molecular model	Number of conformations	Description
X	1	X-ray structure as defined in the text
ref X	1	energy refined X-ray structure: obtained from X by energy refinement
$S[i]$	8	conformation, in which the aromatic ring i is replaced by an equivalent sphere according to the sphere model. The other atoms are in their X-ray positions
ref $S[i]$	8	obtained from $S[i]$ by energy refinement
$R[i, \Delta\chi^2]$	64	conformation, in which the aromatic ring i is treated according to the ring model. The ring is fixed in the rotational state $\Delta\chi_i^2$ and the other atoms are in their X-ray positions. (For each residue we considered the eight rotational states $\Delta\chi_i^2 = 0°$, 22.5°, 45°, . . . 157.5°)
ref $R[i, \Delta\chi^2]$	64	obtained from $R[i, \Delta\chi^2]$ by energy refinement

The flexible sphere model structures ref $S[i]$ (Table 2) were obtained by the application of the above described energy refinement procedures to the model structures $S[i]$, using the parameters of Table 1 for the spheres Y.

The Ring Model

The ring model was selected to study distinct non-equilibrium rotational states of the aromatic rings.

The rigid ring model structures $R[i, \Delta\chi^2]$ (Table 2) were derived from the X-ray structure through rotation of the aromatic ring i about the C_i^β—C_i^γ bond by the torsion angle $\Delta\chi^2$. The energies of these rigid structures were computed with the energy function (1) and the previously introduced energy parameters of Levitt (1974, 1975).

The flexible ring model structures ref $R[i, \Delta\chi^2]$ (Table 2) were obtained by energy refinement of the structures $R[i, \Delta\chi^2]$. The procedure used was similar to that outlined above for the treatment of the X-ray structure, except that the torsion angle χ_i^2 was prevented from drifting during the refinement process. This was achieved with the following parameters for the torsion barrier: $K_\theta(\chi_i^2) = 200$ kcal mole^{-1}; $m = 2$; $\delta = 2 \cdot \chi_i^2(R[i, \Delta\chi^2])$. This choice of parameters led to drifts $|\chi_i^2(\text{ref } R[i, \Delta\chi^2]) - \chi_i^2(R[i, \Delta\chi^2])| \lesssim 1°$. Higher values for $K_\theta(\chi_i^2)$ led to instabilities in the energy refinement process, which resulted in unacceptable conformations from the point of view of stereochemistry. Other than the torsion barrier potential for χ_i^2, the parameters of Levitt (1974, 1975) were used for the refinement of the ring model structures.

Results

From the molecular models described in the preceding section, 146 different conformations were generated and examined. The notation used for the individual molecular species is given in Table 2. One of the conformations considered is the X-ray structure (Deisenhofer and Steigemann, 1975). Eight different species $S[i]$ were obtained by replacement in the X-ray structure of one of the aromatic rings at a time with an equivalent sphere. 64 conformations resulted from the introduction of eight different rotation states for each individual aromatic ring. The atomic coordinates for the eight species $R[i, 0°]$ are identical to those in the X-ray structure, and the 56 conformations $R[i, \Delta\chi^2 \neq 0°]$ differ from the X-ray structure only in the coordinates of the ring carbon atoms δ_1, δ_2, ε_1 and ε_2 of the aromatic residue i. Energy refinement of these 73 conformations yields 73 new species, which will be described in more detail below (Tables 3–5).

Let us first have a closer look at the energy refined X-ray structure of BPTI (ref X). Its energy is 260 kcal/mole lower than that of the X-ray structure (X). The RMS atomic shift ("shift" is defined as the difference in atomic position between the structures X and ref X) is 0.12 Å, which is only slightly larger than the standard deviation of the X-ray analysis (Deisenhofer and Steigemann, 1975). 43% of the atoms were shifted by more than 0.1 Å, 6% by more than 0.2 Å. The largest single

shift of 0.46 Å was experienced by the C^{γ} atom of Lys 46. The atoms with large shifts were distributed essentially uniformly throughout the molecule. On the average, main chain atoms and side chain atoms experienced comparable shifts. The energy difference between X and ref X as well as the RMS atomic shift indicate a close similarity between our energy refined structure and the one of Gelin and Karplus (1975).

Conformational energies E were computed for all the 146 species in Table 2 by evaluating the energy function (1). These conformational energies were used to obtain the energy barriers for rotational motions of the aromatic rings given in Table 3, and the plots of the conformational energy vs. the torsion angle $\Delta\chi_i^2$ of the aromatic rings in the Figures 1 and 2. In the sphere models, the rotation barrier was taken to be the energy difference between $S[i]$ and the X-ray structure, and ref $S[i]$ and the refined X-ray structure, respectively.

$$\Delta E^{\neq}_{\text{rigid}} = E(S[i]) - E(\text{X}) \tag{3}$$

$$\Delta E^{\neq}_{\text{flexible}} = E(\text{ref } S[i]) - E(\text{ref X}). \tag{4}$$

In the ring models we estimated the energy barriers by taking the differences between the maximum and the minimum values among the energies for all the different rotational stages of a given residue i.

$$\Delta E^{\neq}_{\text{rigid}} = \max_{\Delta\chi_i^2} E(R[i, \Delta\chi^2]) - \min_{\Delta\chi_i^2} E(R[i, \Delta\chi^2]) \tag{5}$$

$$\Delta E^{\neq}_{\text{flexible}} = \max_{\Delta\chi_i^2} E(\text{ref } R[i, \Delta\chi^2]) - \min_{\Delta\chi_i^2} E(\text{ref } R[i, \Delta\chi^2]). \tag{6}$$

In addition to the energy barriers thus obtained for the eight aromatics, Table 3 contains the energy barriers for the four tyrosines proposed by Gelin and Karplus (1975) on the basis of a theoretical model which is very similar to our ring model, and the experimental activation parameters for some of the rings (Wagner et al., 1976). It is seen that in the rigid models examined, aromatic ring rotation is strongly hindered. In the flexible theoretical models, the energy barriers are of the same order of magnitude as the experimental values.

The sphere model does not discriminate between different rotational states $\Delta\chi_i^2$. For the ring models, plots of the relative conformational energy ΔE vs. $\Delta\chi_i^2$ were obtained, with ΔE given by

$$\Delta E(\Delta\chi_i^2)_{\text{rigid}} = E(R[i, \Delta\chi^2]) - E(R[i, 0°]) \tag{7}$$

$$\Delta E(\Delta\chi_i^2)_{\text{flexible}} = E(\text{ref } R[i, \Delta\chi^2]) - E(\text{ref } R[i, 0°]). \tag{8}$$

Figures 1 and 2 show that for all the eight aromatics ΔE increases steadily between a torsion angle $\Delta\chi^2_{\text{min}}$ and a torsion angle $\Delta\chi^2_{\text{max}}$. In the rigid model, $\Delta\chi^2_{\text{min}} = 0°$ for all the rings, and $\Delta\chi^2_{\text{max}}$ is near 90°. In the flexible model, $\Delta\chi^2_{\text{min}} = 0°$ for six of the rings and $\approx -20°$ for Tyr 23 and Phe 33, and $\Delta\chi^2_{\text{max}}$ is between 60° and 100° for all the rings. The deviation in the energy refined structures of $\Delta\chi^2_{\text{min}}$ from 0° for two of the aromatics will be further discussed at the end of this section.

Table 3. Energy barriers for intramolecular rotation of the aromatic rings in BPTI

Residue	Calculated energy barriers (kcal mole^{-1})[a]						Experimental parameters (Wagner et al., 1976)			
	Sphere model		Ring model		Gelin and Karplus (1975)			$\Delta G^{\neq}$ (40 °C)	$\Delta H^{\neq}$	$\Delta S^{\neq}$ (e.u.)
	Rigid	Flexible	Rigid	Flexible	Rigid	Flexible				
Tyr 10	57	13	36	17	22	0		$\lesssim 13$[b]		
Tyr 21	170	34	182	25	140	12		$\lesssim 13$[b]		
Tyr 23	122	59	91	16	63	7		14.7	26	35
Tyr 35	169	53	194	35	175	23		15.8	37	68
Phe 4	102	39	57	21			Phe I	$\lesssim 13$[b]		
Phe 22	150	36	163	20			Phe II	13.7	17	11
Phe 33	69	43	39	20			Phe III	$\lesssim 13$[b]		
Phe 45	120	27	109	32			Phe IV	19.7[c]		

[a] It is understood that energies $\Delta E \gtrsim 100$ kcal are to be considered as "high repulsive energies"; quantitative evaluation of such high energies is beyond the scope of the parametrization used in the present study

[b] Only the limiting case of rapid ring rotation was observed in the NMR spectra. The limiting value of $\Delta G^{\neq}$ given here is meant to indicate that the free enthalpy of activation is probably smaller than the value measured for Phe II

[c] This value for $\Delta G^{\neq}$ was obtained at 80°

As was mentionned above, Table 3 indicates that the experimentally observed rotational motions of the aromatics in BPTI could only be understood in a flexible model of the protein. The observation that the energy barriers obtained from the energy refinement agree quite closely with the experimental values then suggested that simulation of the protein flexibility by the conformational changes during the refinement could also give some insight into the mechanistic aspects of the ring rotations. For this we concentrated on the one hand on the displacements of atoms which led to a reorientation of the rotation axis (C_i^{β}—C_i^{γ} bond) relative to the backbone atoms of the aromatic residue i (Table 4), and on the other hand on the displacements experienced by all the atoms within spheres of different radii about the center of the ith ring (Tables 5 and 6). The atomic displacements were studied for the eight refined ring model structures ref $R[i,\Delta\chi^2_{max}]$, where $\Delta\chi^2_{max}$ describes the rotational state of maximum energy for the aromatic ring i, and for the eight refined sphere model structures ref $S[i]$.

Since the bond stretching force constants K_b are very large, the bond lengths are to a good approximation identical in all the conformations studied. Therefore, the orientations of the C_i^{β}—C_i^{γ} bonds relative to the backbone atoms can adequately be described by the bond angles $\tau_i(NC^{\alpha}C')$, $\tau_i(NC^{\alpha}C^{\beta})$ and $\tau_i(C^{\alpha}C^{\beta}C^{\gamma})$, and by the torsion angle χ_i^1. In Table 4 the displacements of the above mentionned bond angles and of χ_i^1 for the sphere model (S) and for the ring model conformation of maxi-

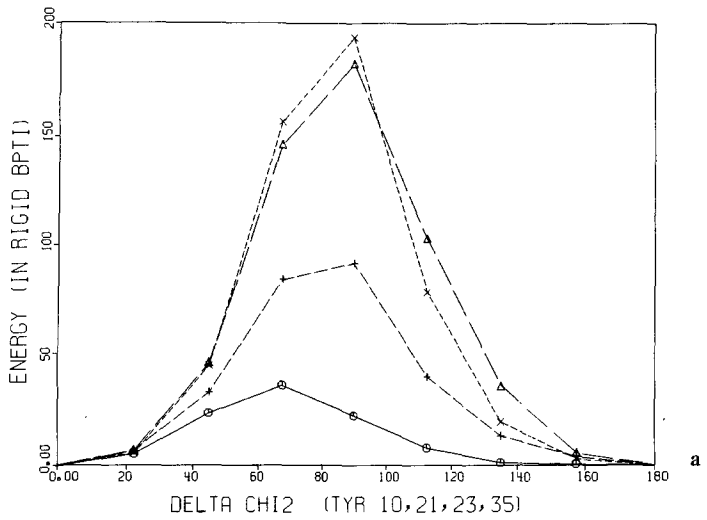

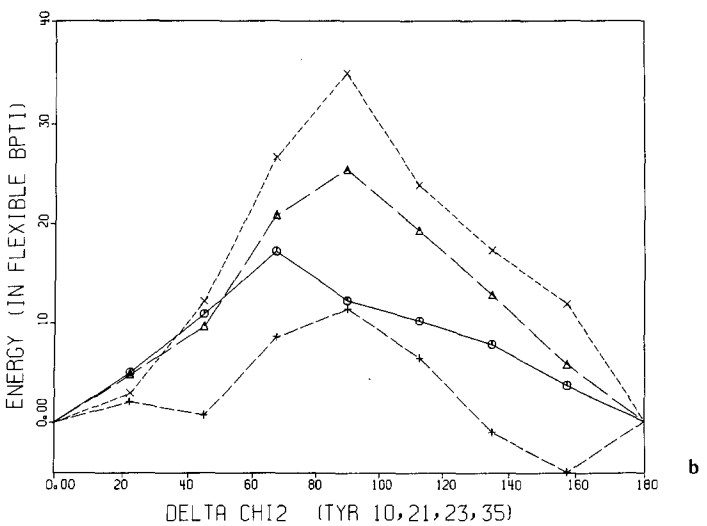

Fig. 1. Conformational energies (in kcal mole^{-1}) of BPTI computed for the different rotation states of the tyrosine rings in the rigid and the flexible molecule. O—O Tyr 10; △---△ Tyr 21; +---+ Tyr 23; ×·····× Tyr 35

mum energy (R) are given for each aromatic residue i. For example for $\Delta\chi_i^1$, the numbers in the table correspond to

$$S\text{: } \Delta\chi_i^1 = \chi_i^1(\text{ref } S[i]) - \chi_i^1(\text{ref X}) \tag{9}$$

$$R\text{: } \Delta\chi_i^1 = \chi_i^1(\text{ref } R[i, \Delta\chi_{\max}^2]) - \chi_i^1(\text{ref X}). \tag{10}$$

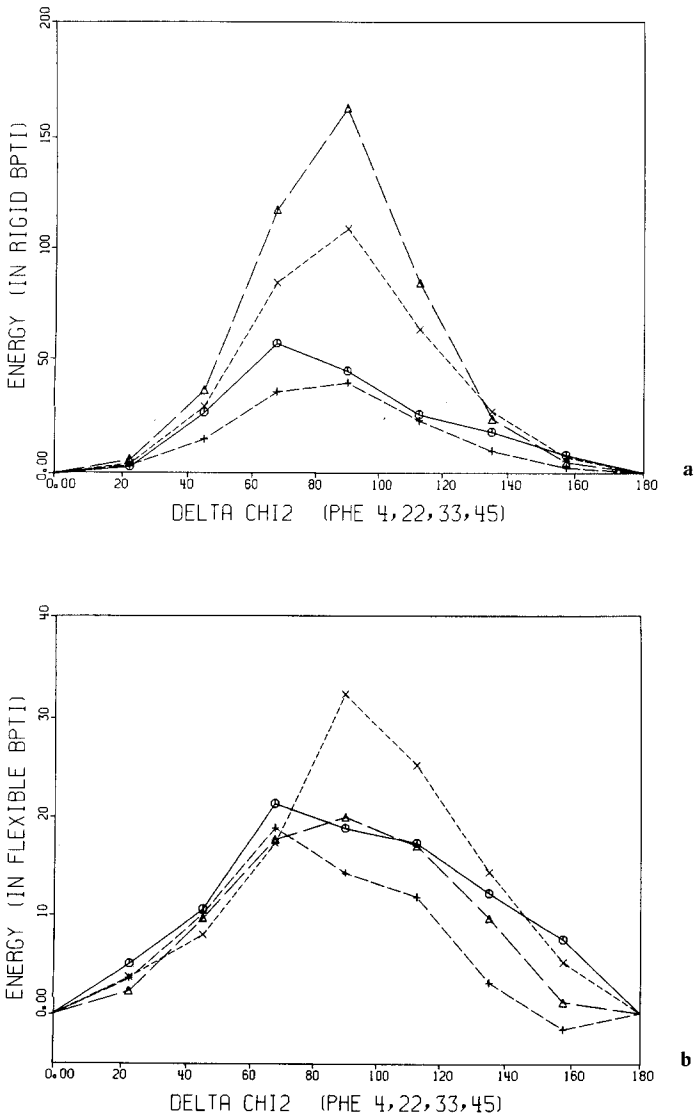

Fig. 2. Conformational energies (in kcal mole^{-1}) of BPTI computed for the different rotation states of the phenylalanine rings in the rigid and the flexible molecule. O—O Phe 4; △– – –△ Phe 22; + – – – + Phe 33; × · · · · · × Phe 45

Corresponding expressions hold for the other parameters. The changes of the spatial orientation of the C_i^β–C_i^γ bonds arising from the energy refinement of the X-ray conformation are also included in Table 4, e.g.

$$\text{X: } \Delta\chi_i^1 = \chi_i^1(\text{ref X}) - \chi_i^1(\text{X}). \tag{11}$$

Table 4. Displacement of the axes of intramolecular rotation of the aromatic rings in BPTI. All angles are given in degrees

Residue	Model[a]	$\Delta\tau_i(NC^\alpha C')$	$\Delta\tau_i(NC^\alpha C^\beta)$	$\Delta\tau_i(C^\alpha C^\beta C^\gamma)$	$\Delta\chi_i^1$
Tyr 10	X	8	−1	1	6
	S	−1	1	0	19
	R	−3	−1	3	5
Tyr 21	X	2	2	1	1
	S	0	−1	2	7
	R	0	1	1	7
Tyr 23	X	−4	2	−1	−7
	S	0	−1	2	1
	R	−3	1	3	7
Tyr 35	X	13	−1	0	14
	S	−1	−3	3	3
	R	−4	−1	4	12
Phe 4	X	1	4	0	1
	S	1	−1	−1	−1
	R	1	−1	0	3
Phe 22	X	5	3	−1	2
	S	1	1	3	−4
	R	0	−1	5	6
Phe 33	X	6	3	−1	5
	S	2	1	1	−4
	R	1	1	4	−9
Phe 45	X	0	2	−2	1
	S	3	−1	−1	−20
	R	0	−2	3	−5

[a] X: Differences between energy refined X-ray structure and the X-ray structure. S: Differences between energy refined structure of sphere model and energy refined X-ray structure. R: Differences between energy refined structure of ring model with χ_i^2 at the position of maximum energy and the energy refined X-ray structure

Overall, Table 4 describes to what extent the rotating aromatic rings evade steric hindrance of the rotational motions by reorientation of the rotation axis.

Additional release of through space interactions may result from displacements of the atoms surrounding the aromatic rings in the protein molecule. The question then arises as to how far such perturbations of the conformation would be propagated in the molecule. We examined the displacements of all the non-hydrogen atoms in BPTI for the sixteen species ref $S[i]$ and ref $R[i, \Delta\chi^2_{max}]$. In Table 5 the atoms are arranged according to the displacement d and the distance r from the center of the aromatic ring i. The displacement d is the absolute value of the vector connecting the positions P_{xyz} of a given atom in the perturbed and unperturbed conformations

$$S\colon\ d = \left|P_{xyz}(\text{ref } S[i]) - P_{xyz}(\text{ref X})\right| \tag{12}$$

$$R\colon\ d = \left|P_{xyz}(\text{ref } R[i, \Delta\chi^2_{max}]) - P_{xyz}(\text{ref X})\right|. \tag{13}$$

Table 5. Displacement of atoms in the structure of BPTI caused by the rotational motion of the aromatic rings. The table gives a survey of the locations of atoms displaced by $d \geqslant 0.1$ Å, and indicates the total number of atoms which were displaced by $d \geqslant 0.02$ Å

Residue	Model[a]	n[b]				
		$d_0 = 0.1$ Å				$d_0 = 0.02$ Å
		$r_0 = 4.5$ Å	$r_0 = 6$ Å	$r_0 = 9$ Å	$r_0 = \infty$	$r_0 = \infty$
Tyr 10	S	6 [8]	14 [27]	15 [72]	15 [445]	45 [445]
	R	6	13	13	13	242
Tyr 21	S	9 [9]	22 [32]	33 [101]	33	83
	R	6	10	16	19	286
Tyr 23	S	12 [12]	28 [41]	45 [130]	46	102
	R	8	11	19	19	101
Tyr 35	S	9 [9]	24 [40]	31 [124]	31	103
	R	8	15	19	20	265
Phe 4	S	9 [9]	26 [34]	34 [93]	36 [446]	83 [446]
	R	4	10	15	17	262
Phe 22	S	6 [8]	19 [40]	30 [112]	30	134
	R	5	7	9	13	278
Phe 33	S	5 [8]	20 [48]	28 [136]	30	94
	R	4	6	8	15	328
Phe 45	S	10 [11]	20 [41]	27 [146]	27	89
	R	6	10	16	22	331

[a] S: Displacements in the energy refined structure of the sphere model from the atom positions in the energy refined X-ray structure (Eq. 12). R: Displacements in the energy refined structure of the ring model with χ_i^2 at the rotation state of maximum energy from the atomic positions in the energy refined X-ray structure (Eq. 13)

[b] n is the number of non-hydrogen atoms located within a sphere of radius r_0 about the center of the aromatic ring considered which are displaced by a distance $d \geqslant d_0$. The number in brackets indicates the total number of (non-hydrogens) atoms within the sphere. The atoms of the aromatic side chain being rotated are not included

The classification of the atoms according to the distance r was made in the unrefined X-ray structure. Table 5 shows that the most important displacements are those that occur in the immediate vicinity of the rotating rings. For example for tyrosine 10 rotation, the sphere model indicates that 45 out of the total of 445 heavy (non-hydrogen) atoms considered are displaced by more than 0.02 Å, and 15 atoms are displaced by more than 0.10 Å. Out of a total of 72 atoms located within 9 Å from the center of the Tyr 10 ring, 15 are displaced by more than 0.10 Å. Within the spheres of radius 6 Å and 4.5 Å, the respective numbers are 14 of 27, and 6 of 8 atoms. Quite generally one finds in Table 5 that within the sphere with radius 4.5 Å, almost all of the atoms are displaced in the sphere model calculations, and significantly more than half of the atoms are also displaced in the ring model calculations. Other results (not shown in the tables) indicate very clearly that almost all of the displacements greater than 0.1 Å observed for atoms with $r \gtrsim 5$ Å can be under-

Table 6. Displacement of atoms in the structure of BPTI caused by the rotational motion of the aromatic rings. The table describes the location relative to the center of the rotating ring of the most extensively displaced atoms, and indicates the root mean square (RMS) displacement for all the atoms in the molecule

Residue	Model[a]	n[b]									RMS of displacements (in Å)
		$r_0 = 4.5$ Å			$r_0 = 6$ Å			$r_0 = \infty$			
		$0.2 > d \geqslant 0.1$	$0.5 > d \geqslant 0.2$	$d \geqslant 0.5$ Å	$0.2 > d \geqslant 0.1$	$0.5 > d \geqslant 0.2$	$d \geqslant 0.5$ Å	$0.2 > d \geqslant 0.1$	$0.5 > d \geqslant 0.2$	$d \geqslant 0.5$ Å	$r_0 = \infty$
Tyr 10	S	2	3	1	7	6	1	8	6	1	0.05
	R	3	3	0	10	3	0	10	3	0	0.05
Tyr 21	S	2	6	1	9	10	3	15	15	3	0.10
	R	2	3	1	3	6	1	11	7	1	0.06
Tyr 23	S	3	8	1	15	12	1	30	15	1	0.08
	R	3	4	1	5	5	1	13	5	1	0.05
Tyr 35	S	3	4	2	12	10	2	16	13	2	0.09
	R	2	5	1	4	10	1	8	11	1	0.07
Phe 4	S	3	3	3	13	9	4	22	10	4	0.09
	R	1	2	1	5	4	1	12	4	1	0.06
Phe 22	S	1	1	4	9	6	4	18	8	4	0.09
	R	0	2	3	2	2	3	6	4	3	0.06
Phe 33	S	1	4	0	14	6	0	23	7	0	0.06
	R	1	3	0	2	4	0	11	4	0	0.05
Phe 45	S	7	2	1	14	5	1	17	9	1	0.06
	R	2	4	0	5	5	0	17	5	0	0.05

[a] S: Displacements in the energy refined structure of the sphere model from the atom positions in the energy refined X-ray structure (Eq. 12). R: Displacements in the energy refined structure of the ring model with χ_i^2 at the rotation state of maximum energy from the atomic positions in the energy refined X-ray structure (Eq. 13)

[b] n is the number of non-hydrogen atoms located within a sphere of radius r_0 about the center of the aromatic ring considered, for which the displacement d is within the indicated range of values

stood in terms of secondary effects resulting from the propagation through the covalent bonds (up to about 5 bonds) of the perturbations primarily experienced by an atom located within a sphere of radius $r_0 \approx 5$ Å about the ring center.

Table 6 describes in more detail the spatial distribution of the largest atom displacements, i.e. those with $d \geqslant 0.1$ (Table 5), in the BPTI structure. The table considers the atoms within two spheres with radii $r_0 = 4.5$ Å and 6.0 Å about the center of the rotating ring, and the total number of atoms in the molecule. It distinguishes between atoms displaced by 0.5 Å or more, those with 0.5 Å $> d \geqslant 0.2$ Å, and those with 0.2 Å $> d \geqslant 0.1$ Å. The table reemphasizes the conclusion from Table 5 that the predominant number of large atom displacements occur in the immediate vicinity of the rotating ring. For example in the ring model, all the displacements by $d \geqslant 0.5$ Å occur for atoms which are within a distance of 4.5 Å from the ring center; essentially all the displacements between 0.2 and 0.5 Å are within a distance of 6.0 Å. The Table 6 gives further the RMS displacement for all the atoms of BPTI caused by the rotations of the individual aromatic rings.

All the displacements in the Tables 4, 5 and 6 were obtained as the differences between the perturbed energy refined conformations (ref $S[i]$, ref $R[i, \Delta\chi^2_{\max}]$) and the unperturbed energy refined conformations (ref X). In this way the atomic shifts between X and ref X, which were already briefly discussed earlier in this section, have been separated from the atomic displacements resulting from the rotational motions of the aromatic rings. This was required since the atomic shifts between X and ref X result primarily from systematic inconsistencies between these two conformations. This includes that the energy function used in the refinement corresponds at best to a reasonable approximation of the situation in the real molecule, and that the energy refinement was done on the isolated BPTI molecule; the experimental X-ray data correspond of course to BPTI in the crystal lattice. Also, the crystallographic refinement used to obtain the conformation X (Deisenhofer and Steigemann, 1975) tends to concentrate steric strain in certain conformational parameters while the strain is nearly evenly distributed in the energy refined species. For example, in the conformation X a lot of unresolved strain is concentrated in the angles $\tau(NC^{\alpha}C')$. For Tyr 35 this angle has a value of 100°, which differs by more than 10° from the equilibrium bond angle $\tau^0(NC^{\alpha}C')$ used in the energy function (1). Through energy minimization, this strain is relieved by an increase of $\tau(NC^{\alpha}C')$ (Table 4), and as a consequence of the resulting new steric situation, one observes also a sizeable change of χ^1 for tyrosine 35 (Table 4).

In this context, an additional comment is called for concerning the observation that in the energy refined ring model structures (Figs. 1 and 2) $\Delta\chi^2_{\min} \neq 0°$ for Tyr 23 and Phe 33. It is quite conceivable that the energetically most favorable rotation states of some of the aromatic rings in the isolated BPTI molecule could be different from the equilibrium rotation states observed in the X-ray data. However, since the refinement procedures used (Levitt 1974, 1975) consider only conformations which deviate from the initial model conformation by small variations of individual local structural parameters, the refinement of the X-ray structure did not result in conformations with largely different ring rotation states. For the two rings in question, the variation of χ^2_{23} and χ^2_{33} between X and ref X was actually smaller than 2°. Thus, even though the energies of the conformations ref $R[i, \Delta\chi^2]$ were referred to ref $R[i, 0°]$, the systematic inconsistencies between the X-ray structure in the crys-

tal and the molecular models for isolated BPTI are still manifested in the data of Figures 1 and 2.

Discussion

In the preceding sections, several different molecular models (Table 2) were used to investigate structural and energetic aspects of the experimentally observed (Wüthrich and Wagner, 1975; Wagner et al., 1976) intramolecular rotation of the aromatic rings in the globular conformation of the basic pancreatic trypsin inhibitor BPTI. The results obtained, i.e. conformational energies for BPTI molecules with individual aromatic rings in variable rotation states χ_i^2, activation energies for rotational motions of the aromatic rings and parameters describing the perturbations of the molecular structures by the rotating rings, were collected in the Figures 1 and 2 and the Tables 3–6. On the basis of these data, this discussion focuses mainly on three themes. These are a comparison and evaluation of the results obtained with the use of the different molecular models, consideration of the mechanistic aspects of ring rotation and some general conclusions which may be drawn from the investigations presented in this paper.

Significance of the Different Molecular Models

All the molecular models used (Table 2) have in common that the dynamics of ring rotation are not explicitely accounted for. The sphere models represent a static situation where the aromatic ring i in question is replaced by an equivalent sphere representing the space occupied by the ensemble of all the rotational states χ_i^2, and the ring models represent different static situations characterized by fixed rotation states χ_i^2 of the ring considered. We will now first discuss some qualitative conclusions which result from these static models. Next, relations between the static models used and the dynamics of ring rotation will be considered, the influence of mutual interactions between different rotating rings in the BPTI molecule will be assessed and the conformational energies obtained from the different models will be critically reviewed.

The ring models discriminate between the relative conformational energies of molecular species containing the ring i in different rotation states χ_i^2. Figures 1 and 2 show an important qualitative result of both the rigid model and flexible model calculations; among the different static situations considered, the conformational energies increase continuously between two rotation states χ^2_{min} and χ^2_{max}, which are near the equilibrium state with $\Delta\chi_i^2 = 0°$ observed in the crystal structure and near $\Delta\chi_i^2 = 90°$, respectively. From the shape of the curves in Figures 1 and 2 and calibrating the vertical scales of the figures by equating $E(\Delta\chi_i^2)_{\text{max}}$ with the experimental values for the activation enthalpies of approximately 10–40 kcal mole^{-1} (Table 3), one finds that for the individual rings the thermally populated rotation states at ambient temperatures are confined to the range $\Delta\chi_i^2 = \Delta\chi^2_{\text{min}} \pm 20°$. On the one hand this agrees quite closely with the experimental temperature factors in the crystal structure. The average temperature factors for the four ring carbon atoms δ_1,

δ_2, ε_1 and ε_2 of the individual rings are 16.3 ± 2.5, 11.1 ± 1.3, 12.3 ± 1.7 and 11.8 ± 1.7 Å^2 for the phenylalanyl residues 4, 22, 33 and 45, respectively, and 18.1 ± 2.4, 12.1 ± 1.8, 9.5 ± 1.7 and 12.2 ± 0.7 Å^2 for the tyrosines 10, 21, 23 and 35, respectively. These temperature factors correspond to root mean square variations of the atomic coordinates of approximately 0.30 Å to 0.45 Å; for the atoms δ_1, δ_2, ε_1 and ε_2 this is equivalent with variations of χ_i^2 of the order < 25°. On the other hand, the Figures 1 and 2 indicate that the rotational motions of the aromatic rings about the C_i^β–C_i^γ bonds should essentially consist of "180° flips", since appreciable population of any of the intermediate states can be excluded. This coincides with the conclusions from ^{1}H NMR studies of these ring rotations (Wüthrich and Wagner, 1975; Wagner et al., 1976). This qualitative analysis of the data in Figures 1 and 2, which did not make use of the calculated absolute values for the conformational energies, thus provides also an illustration of the compatibility of the X-ray data for BPTI single crystals (Deisenhofer and Steigemann, 1975) and the NMR data for aqueous BPTI solutions (Wagner et al., 1976).

The ring models and sphere models are related to two limiting dynamic situations. If the ring rotations about the C^β–C^γ bond were rapid compared to the rates of atom displacement in their environment which are required to make ring rotation sterically possible (Tables 5 and 6), the sphere models would probably be a quite realistic representation of the actual situation. If the ring rotations were slow compared to the atom displacements in their environment, the ring models would correspond to a more realistic representation. The presently available experimental observations provide no clue as to which of these limiting cases might prevail; only the frequency of the 180° flips of the aromatic rings but not the actual rate of displacement of the atom positions δ_1, δ_2, ε_1 and ε_2 during the flipping motions are manifested in the NMR spectra. A priori, one would probably anticipate an intermediate situation with comparable rates of atom displacements for the different intramolecular motions. It is then of particular interest that the structural implications of ring rotation, which will be discussed in more detail below, are very similar for the two models chosen to represent the two limiting dynamic situations.

In the investigations presented in this paper, both the ring models and the sphere models do not account for concerted rotational motions of two or more aromatic rings. It appears that the inherent assumption of independent rotational motions of the individual aromatics gives a reasonable representation of the actual situation in BPTI. As mentioned above, for each individual ring i only rotation states near the equilibrium situation $\Delta\chi_i^2 = 0°$ are appreciably populated at ambient temperatures. It is therefore highly unlikely that any two rings are simultaneously in rotation states with $|\Delta\chi_i^2| \gtrsim 20°$. The aromatic rings in BPTI are also rather well separated from each other. In the X-ray structure there are only eight δ- or ε-atoms of neighboring rings within the spheres of radius $r_0 = 6$ Å about the centers of the individual rings i (compare with the total number of nearby atoms in Table 5). Five of these close distances are between Phe 22 and Phe 33, with $r = 4.6$, 4.9, 5.5, 5.6 and 5.9 Å, two are between Phe 33 and Tyr 35, with $r = 5.7$ and 5.8 Å, and the atom ε_1 of Phe 45 is 5.4 Å away from the ring center of Phe 4. Furthermore, inspection of the atom displacements by the rotating rings showed that in the flexible ring model structures no atom of a neighboring aromatic side chain was displaced by 0.1 Å or more. In the flexible sphere model structures, only two such atom displacements were observed;

rotation of Phe 33 caused displacements of Tyr 35 C^{β} by ≈ 0.2 Å and of Tyr 35 C^{γ} by ≈ 0.1 Å. (Compare with the total number of displaced atoms in Tables 5 and 6.)

The energy barriers calculated with the flexible ring model correspond quite satisfactorily with the experimental parameters (Table 3). Combined with the above mentioned qualitative agreement of the data in Figures 1 and 2 with X-ray and NMR data, we take this as an indication that the information on mechanistic aspects of ring rotation derived from the same model structures (Tables 4—6) should be quite meaningful. On similar grounds we would expect that the flexible sphere model with the parameters of Table 1 should tend to overemphasize the perturbations of the molecular structure by the ring rotations, since the energy barriers calculated with this model are rather high (Table 3). More detailed interpretations of the calculated energies are not envisaged. It should be evident from the previous discussion that much care has to be taken in the appreciation of these values; this is reemphasized by the comparison of our ring model data with those of Gelin and Karplus (Table 3), which were calculated on the basis of a very similar model.

An additional comment is called for concerning the conformational energies of the rigid model structures. The rather high energy barriers (Table 3) are in all cases mainly due to a small number of short interatomic contacts; for most of the rings, one or two pairs of atoms made the dominant contribution. This is quite clearly seen by comparing the data of Figures 2 and 3. The data in Figure 3 were obtained by a very simple minded approach: the individual aromatic rings in the X-ray structure were rotated in steps of $\Delta\chi_i^2 = 22.5°$ and the nearest interatomic distances for each rotation state were recorded. In Figure 3 the shortest interatomic distance for each of the four phenylalanine rings is plotted vs. $\Delta\chi_i^2$. It is readily apparent that the qualitative features of these curves correspond quite closely to those in Figure 2. It

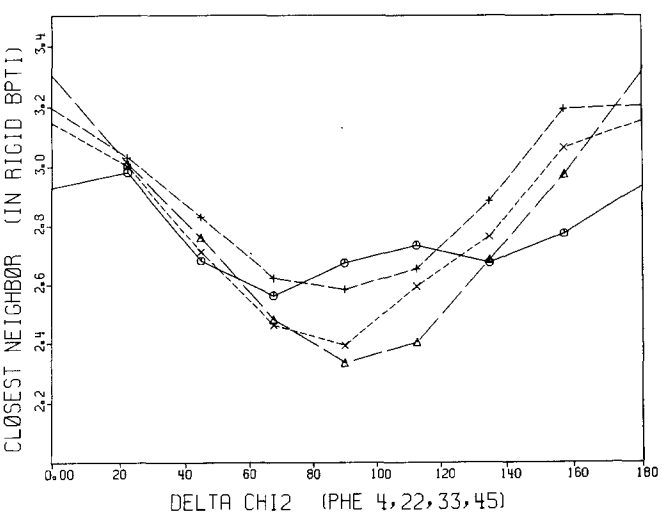

Fig. 3. Closest through space interatomic distances (in Å) between any of the ring carbon atoms of the aromatic ring considered and any of the atoms in the rest of the molecule. O—O Phe 4; △– –△ Phe 22; + – – – + Phe 33; × · · · · · × Phe 45

may be added that similar curves were obtained for the four tyrosines in BPTI, and that somewhat smoother curves resulted when a suitable combination of the three shortest contacts per ring was plotted vs. $\Delta\chi_i^2$. The dominant role of the non-bonded repulsive terms in the energy function (1) became even more pronounced when the "Hydro" option in Levitt's program (1975) was used to explicitely include the hydrogen atoms in the molecular structures. The rigid model calculations then gave energy barriers in the range from approximately 600 kcal mole^{-1} to 700,000 kcal mole^{-1} for the eight aromatic rings. It was readily apparent that these extremely high energies for some of the non-equilibrium rotation states χ_i^2 were a consequence of extremely short contacts between a small number of atoms: in most cases one or two pairs of hydrogen atoms were located at distances of the order 0.65–1.0 Å. These "forbidden" short contacts would of course be eliminated in the first few cycles of energy refinement.

Structural Aspects of Ring Rotation

Two significant features of the ring rotations were revealed by the foregoing discussion of the different models, i.e. that the rotational motions consist essentially of 180° flips about the C_i^β–C_i^γ bonds and that the increased conformational energies of molecular species containing non-equilibrium rotation states of aromatic rings arise primarily from non-bonded repulsive interactions of ring atoms with their immediate environment. In the following the impact of the non-bonding interactions on the overall molecular structure of BPTI will be investigated. It may be mentioned beforehand that qualitatively very similar conclusions were reached for the flexible sphere model structures and the flexible ring model structures. It appears therefore that essentially identical mechanistic and structural features should prevail for the limiting dynamic situations represented by the two models.

In the flexible molecular structures considered, the steric strain resulting from near interatomic contacts with the rotated ring i can be released by changing the axis of rotation C_i^β–C_i^γ and by displacement of atoms surrounding the aromatic ring. In Table 4, the displacements of the rotation axes are characterized by the variations of three bond angles τ_i and the torsion angle χ_i^1. It is seen that in the energy refinement of the sphere model structures, the variations of the bond angles $\tau_i(NC^\alpha C')$, $\tau_i(NC^\alpha C^\beta)$ and $\tau_i(C^\alpha C^\beta C^\gamma)$ are all smaller than or equal to 3°. In the ring model structures, $\tau_{22}(C^\alpha C^\beta C^\gamma)$ varied by 5°, three bond angles varied by 4° and all the other variations were smaller than or equal to 3°. Variation of $\tau_i(C^\alpha C^\beta C^\gamma)$ by 3° corresponds to displacements of C_i^ζ by approximately 0.25 Å and C_i^γ by approximately 0.10 Å. In the sphere model structures, rather large variations $\Delta\chi_i^1 = 19°$ and $-20°$ were obtained for Tyr 10 and Phe 45; these variations correspond to displacements of C_i^ζ by $\sim$ 1.5 Å and C_i^γ by $\sim$ 0.5 Å. For the other six rings, $|\Delta\chi_i^1| \leqslant 7°$, which corresponds to displacements of C_i^ζ and C_i^γ by $\lesssim$ 0.55 Å and $\lesssim$ 0.20 Å, respectively. In the ring model structures we have that $|\Delta\chi^1| \leqslant 7°$ for six of the rings, the two extreme values being $\Delta\chi_{35}^1 = 12°$ and $\Delta\chi_{33}^1 = -9°$. For the individual atoms, the displacements corresponding to variations of the different angles may in part add up and in part cancel each other. The calculations with the different model structures showed that the resulting overall displacements for atoms of the rotated

rings are between 0.1 Å and 0.6 Å, with two extreme displacements in the sphere model for C^{ζ}_{10} and C^{ζ}_{45} of $\sim$ 1.1 Å and $\sim$ 1.5 Å, respectively. These perturbations are attenuated in the propagation through the covalent bonds which link the aromatic rings with the polypeptide backbone. The displacements of the atoms C^{α}_i, N_i and C'_i are $\lesssim$ 0.2 Å.

The behavior of the atoms surrounding the aromatic rings in the globular BPTI structure is characterized by the data in Tables 5 and 6. In the sphere model structures, between 45 and 134 atoms were displaced by $\geqslant$ 0.02 Å through the rotations of the individual rings; between 15 and 46 atoms per ring were displaced by $\geqslant$ 0.10 Å. The corresponding numbers for the sphere model structures are 101—331 atoms per ring displaced by $\geqslant$ 0.02 Å and 13—22 atoms displaced by $\geqslant$ 0.1 Å. Table 5 shows further that the atom displacements by $\geqslant$ 0.1 Å are clustered in the immediate vicinity of the rotated ring, both in the sphere model structures and the ring model structures. This clustering around the rotated rings is even more pronounced when the atoms are classified with the limits $d \geqslant 0.5$ Å and $d \geqslant 0.2$ Å (Table 6). It is further seen from Table 6 that very few atoms are displaced by 0.5 Å or more, i.e. between 0 and 4 atoms for rotation of the individual rings in both the sphere model structures and the ring model structures; 3—18 atoms per ring are displaced by $\geqslant$ 0.2 Å.

In conclusion, the molecular models investigated indicate that the aromatic rings in BPTI can rotate about the C^{β}—C^{γ} bonds without causing extensive perturbations of the protein structure. The steric strain which would arise from short interatomic contacts in the rigid X-ray structure containing non-equilibrium rotation states (S[i] and R[i, $\Delta\chi^2$] in Table 2) is avoided by displacement of both the rotation axes C^{β}_i—C^{γ}_i and the atoms of the ring environments. Extensive atom displacements are essentially restricted to the rotating aromatic ring itself and the atoms within a sphere with radius $r_0 = 6$ Å about the center of the ring. Besides those of the rotated aromatic ring, very few atoms are displaced by $\geqslant$ 0.2 Å. Ring rotation thus appears to cause only strictly localized perturbations of the protein conformation.

Conclusions

Despite its small size, which allowed quite extensive studies without prohibitively high expense of computer time, BPTI should be a valid model for studies of the molecular dynamics of globular proteins. Compared to other small and medium sized protein molecules, the backbone conformation of BPTI in solution is outstandingly rigid (Masson and Wüthrich, 1973; Karplus et al., 1973), and a rigid structure is also indicated by the small temperature factors of the X-ray data (Deisenhofer and Steigemann, 1975). The results of the present model investigation of BPTI should thus quite generally be applicable for phenylalanyl and tyrosyl residues in globular proteins. This appears to be corroborated by ^{1}H NMR observations in several different proteins. Even though transitions from slow to rapid ring rotation could not be observed in any of these proteins, certain NMR spectral features of lysozyme (Campbell et al., 1975), cytochrome c (Dobson et al., 1975; Wüthrich, 1976) and cytochrome b_5 (Keller and Wüthrich, 1976) can in analogy to the BPTI data be taken as evidence for rapid rotation of individual phenylalanine and tyrosine rings.

Inspection of molecular models implies that rotational motions about the C^{β}–C^{γ} bond are to be expected also for histidyl residues, unless the imidazole ring is fixed in space by specific interactions with its environment in the protein. For tryptophanyl residues, however, rotation about the C^{β}–C^{γ} bond in the interior of globular proteins seems less likely; the resulting asymmetric "flag motions" of the indole ring would necessarily cause major rearrangements of the protein conformation, with atom displacements which would by far exceed those encountered in Table 6. The observation of rotating aromatic rings (Wüthrich and Wagner, 1975; Wagner et al., 1976) gives direct evidence that vibrations of considerable amplitude traverse protein molecules. This might be of particular relevance for enzymatic activities of protein molecules, which appear to depend critically on the mobility of catalytic site residues (Bode et al., 1975). Enzymatic activity may thus be affected by changes of the vibrational modes of the molecular structure, which could be influenced by local structural changes far away from the catalytic site which do not necessarily perturb the average molecular conformation of the rest of the molecule observed by X-ray methods. Enzymes from thermophilic organisms, which can in many cases be investigated over the entire temperature range from 5–90° (Singleton and Amelunxen, 1973; Stellwagen et al., 1973), might be particularly suitable for future studies of such phenomena. It appears quite conceivable that the temperature dependence of the enzymatic activity could be affected by the temperature dependent rates and amplitudes of intramolecular segmental motions in localized regions of the protein molecules. The experiments with BPTI at temperatures between 5° and 90° (Wüthrich and Wagner, 1975; Wagner et al., 1976) show that the aromatic rings are suitable NMR probes indicating the occurrence of time dependent perturbations of protein conformations.

Acknowledgements. Financial support by the Schweizerischer Nationalfonds (project 3.1510.73) is gratefully acknowledged.

References

Bode, W., Schwager, P., Huber, R.: Structure of the complex between trypsin and trypsin inhibitor. IV. Strong specific protein-protein interaction and catalysis. Proceedings of the 10th FEBS Meeting, pp. 3–20 (1975)

Campbell, I. D., Dobson, C. M., Williams, R. J. P.: Proton magnetic resonance studies of the tyrosine residues of hen lysozyme-Assignment and detection of conformational mobility. Proc. roy. Soc. B **189**, 503–509 (1975)

Deisenhofer, J., Steigemann, W.: Crystallographic refinement of the structure of bovine pancreatic trypsin inhibitor at 1.5 Å resolution. Acta Cryst. **B31**, 238–250 (1975)

Diamond, R.: A real-space refinement procedure for proteins. Acta Cryst. **A27**, 436–452 (1971)

Diamond, R.: Real-space refinement of the structure of hen egg-white lysozyme. J. molec. Biol. **82**, 371–391 (1974)

Dobson, C. M., Moore, G. R., Williams, R. J. P.: Assignment of aromatic amino acid PMR resonances of horse ferricytochrome c. FEBS Lett. **51**, 60–65 (1975)

Gelin, B. R., Karplus, M.: Side chain torsional potentials and motion of amino acids in proteins: Bovine pancreatic trypsin inhibitor. Proc. nat. Acad. Sci. Wash. **72**, 2002–2006 (1975)

Huber, R., Kukla, D., Rühlmann, A., Steigemann, W.: Pancreatic trypsin inhibitor (Kunitz). Cold Spr. Harb. Symp. quant. Biol. **36**, 141–150 (1971)

Karplus, S., Snyder, G. H., Sykes, B. D.: A nuclear mangetic resonance study of bovine pancreatic trypsin inhibitor. Tyrosine titrations and backbone NH groups. Biochemistry **12**, 1323–1329 (1973)

Keller, R., Wüthrich, K.: Unpublished data on cytochrome b_5 (1976)

Levitt, M.: Energy refinement of hen egg-white lysozyme. J. molec. Biol. **82**, 393–420 (1974)

Levitt, M.: Energy refinement procedures, including testdeck. Personal communication (1975)

Levitt, M., Lifson, S.: Refinement of protein conformations using a macromolecular energy minimization procedure. J. molec. Biol. **46**, 269–279 (1969)

Masson, A., Wüthrich, K.: Proton magnetic resonance investigation of the conformational properties of the basic pancreatic trypsin inhibitor. FEBS Lett. **31**, 114–118 (1973)

Singleton, R., Amelunxen, R. E.: Proteins from thermophilic microorganisms. Bact. Rev. **37**, 320–342 (1973)

Stellwagen, E., Cronlund, M. M., Barnes, L. D.: A thermostable enolase from the extreme thermophile *Thermus aquaticus*. Biochemistry **12**, 1552–1565 (1973)

Wagner, G., De Marco, A., Wüthrich, K.: Dynamics of the aromatic amino acid residues in the globular conformation of the basic pancreatic trypsin inhibitor (BPTI) I. ^{1}H NMR studies. Biophys. Struct. Mechanism **2**, 139 (1976)

Wüthrich, K.: The heme groups as natural NMR probes of hemoprotein conformation. Proceedings of the 1st Taniguchi Symposium on Biophysics, Kyoto, November 1975. In press (1976)

Wüthrich, K., Wagner, G.: NMR investigations of the dynamics of the aromatic amino acid residues in the basic pancreatic trypsin inhibitor. FEBS Lett. **50**, 265–268 (1975)

Received April 8, 1976